Available online at www.sciencedirect.com
SCIENCE DIRECT®
Catalysis Today 111 (2006) 354–360
CATALYSIS TODAY
www.elsevier.com/locate/cattod

Oxidative dehydrogenation of methanol over a ruthenium-containing polyoxomolybdate supported on metal oxides chemically modified with silane coupling agent

Tomohiro Oonaka, Keiji Hashimoto, Hiroshi Kominami *, Yoshiya Kera, Yoshio Matsubara

Interdisciplinary Graduate School of Science and Technology, Kinki University, 3-4-1 Kowakae, Higashiosaka, Osaka 577-8502, Japan

Received 10 May 2005; accepted 13 October 2005
Available online 15 December 2005

Abstract

A salt of ruthenium-containing polyoxomolybdate anion ($[Ru_2Mo_{14}O_{50}]^{10-}$ or $[Ru_2Mo_{14}O_{52}]^{14-}$; Ru_2Mo_{14}) was synthesized by mixing ruthenium chloride and sodium molybdate in a buffer solution (acetic acid–ammonium acetate) at pH 5. The polyanion, Ru_2Mo_{14}, was loaded on a silica carrier chemically modified with a silane coupling agent having a 1,2-diaminoethyl group (DAPS–SiO_2). X-ray diffraction, FT-IR and surface area measurements revealed that Ru_2Mo_{14} was highly dispersed on DAPS–SiO_2 up to 20 wt.% loading. The highly dispersed Ru_2Mo_{14} exhibited a high level of activity for oxidative dehydrogenation of methanol to formaldehyde with a high selectivity, whereas combustion of methanol occurred on the bulky salt of Ru_2Mo_{14} and ruthenium catalyst supported on a SiO_2 carrier.
© 2005 Elsevier B.V. All rights reserved.

Keywords: Ruthenium molybdenum polyoxometalate; Methanol oxidation; Silane coupling agent

1. Introduction

Metal-containing polyoxometalates have been known as multi-functional catalysts having high levels of activity in both oxidative and acid-catalyzed reactions. Much interest has also been shown in the relations between their conformation and characteristics. Each of the polyoxometalates consists of metal oxide anions, MO_6 ($M = W^{6+}$, Mo^{6+}, V^{5+}, etc.), and has a characteristic crystal structure [1–10]. These polyoxometalates regiospecifically substitute their anions for some other metal ions or form a bond between the anions and other metal ions [1].

We have studied polyoxometalates containing phosphorus (as phosphate), transition metal ions and lanthanide ions [11–20]. In our previous study [17], it was revealed that substitution of molybdate anion for transition metal ions such as iron (Fe), cobalt (Co) and nickel (Ni) improved the mobility of lattice oxygen and decreased the acidity of the polyoxomolybdates. Loading these polyoxomolybdates on supports chemically modified with silane coupling agents remarkably increased the catalytic activity [17]. It is therefore expected that substitution of molybdate anion for ruthenium (Ru) ion will also improve oxygen mobility because of the changeable valance and larger electronegativity and ion radius of Ru compared with those of Fe, Co and Ni. However, there have been few studies on heteropolyoxomolybdates containing Ru [21,22]. It has recently been reported that heteropolyoxotungstates containing Ru ions were effective for oxidation of hydrocarbons with dioxygen (O_2) and a good acid-catalyst [23–25].

We have attempted to prepare a new type of heteropolyoxomolybdate containing Ru and then to apply it to the oxidation of methanol to formaldehyde, the reaction of which has been used as a catalyst surface probe because of its structurally sensitive characteristics [26–28] and has been extensively investigated as an important and interesting process in industrial chemistry [29]. In this paper, we report (1) synthesis of Ru-containing polyoxomolybdate, (2) high levels of activity and selectivity of the polyoxomolybdate loaded on a silica (SiO_2) carrier for this reaction and (3) efficiency of the modification of a SiO_2 carrier with a silane coupling agent.

* Corresponding author. Fax: +81 6 727 4301.
E-mail address: hiro@apch.kindai.ac.jp (H. Kominami).

0920-5861/$ – see front matter © 2005 Elsevier B.V. All rights reserved.
doi:10.1016/j.cattod.2005.10.047

2. Experimental

2.1. Materials

Ruthenium trichloride *n*-hydrate, $RuCl_3 \cdot nH_2O$ (n = ca. 3) and sodium molybdate dihydrates, $Na_2MoO_4 \cdot 2H_2O$, were of commercial reagent grade and used without further purification for preparation of Ru-containing polyoxomolybdate. As the catalyst carrier, SiO_2 (Aldrich, no. 643; surface area, 266 $m^2\ g^{-1}$) was used.

2.2. Preparation of a salt of Ru-containing polyoxomolybdate

A salt of Ru-containing polyoxomolybdate was prepared as follows: 6.3 g sodium molybdate was dissolved in an acetic acid–ammonium acetate (2:1) buffer solution (40 cm^3) kept at pH 5.0, and then 5 cm^3 of ruthenium trichloride *n*-hydrate (1.0 g) aqueous solution was added dropwise with vigorous stirring. The solution was reacted at 353 K for 1 h and was then filtered to remove insoluble species. The filtered solution was allowed to stand at room temperature for 10 days to obtain needle-like and dark-brownish crystals. The crystals were purified once by a recrystallization method. The atomic ratio of the product was determined to be Na:N:Ru:Mo = 4:1:1:7 using inductively coupled plasma emission spectroscopy (ICP, Na, Ru and Mo, Shimadzu ICPS-1000III) and elemental analysis (N, reported from Galbraith Laboratory Inc., USA). Hereafter, the Ru-containing polyoxomolybdate anion constituting the product crystals is abbreviated as Ru_2Mo_{14}.

2.3. Modification of SiO_2 carrier with a silane coupling agent and loading Ru_2Mo_{14} on the modified SiO_2

The carrier (SiO_2), 2 g, was pretreated in a nitrogen stream at 383 K for 1 h, and then 20 cm^3 of toluene solution of *N*-(2-aminoethyl)-3-aminopropyl trimethoxysilane (Shinetsu Chem. Co. Ltd.; DAPS), the amount of which could cover triplicately the surface of SiO_2, was added; the modification was carried out under the refluxing condition of toluene at 403 K for 2 h according to the literature [15]. The Ru_2Mo_{14} anion was introduced onto the surface of the modified SiO_2 (DAPS–SiO_2) by an equilibrium adsorption method as follows. The DAPS–SiO_2 was suspended in 10 cm^3 of distilled water with stirring for 2 h, and pH of the suspension was adjusted to 4.0 with 1 M HNO_3 solution, and then the solution of the salt of Ru_2Mo_{14} was added to the suspension to make the Ru_2Mo_{14} anions fully absorb on the DAPS–SiO_2. The Ru_2Mo_{14}-loaded DAPS–SiO_2 was separated from the mixture by centrifugation. The amounts of Ru_2Mo_{14} loaded and the atomic ratio (Mo/Ru) were determined by ICP: the amount of Ru_2Mo_{14} loaded on DAPS–SiO_2 was determined from differences in the concentrations of Ru and Mo before and after adsorption. Samples (Ru_2Mo_{14}/DAPS–SiO_2) having various Ru_2Mo_{14} contents were obtained by changing the initial concentration of the salt of Ru_2Mo_{14}. The loaded samples were calcined under air at 623 K for 2 h to remove the organic moieties of DAPS and then used as catalysts for methanol oxidation. The calcined samples are abbreviated as Ru_2Mo_{14}/DC–SiO_2.

2.4. Characterizations

FT-IR spectra of the salt of Ru_2Mo_{14}, DAPS–SiO_2, Ru_2Mo_{14}/DAPS–SiO_2 and Ru_2Mo_{14}/DC–SiO_2 were recorded by the usual disk method on a Shimadzu FT-IR-8300 spectrometer with 4 cm^{-1} resolution and 64 scans. The specific surface area of each sample was determined by the usual BET single-point method using nitrogen (N_2) uptake at 77 K (Shimadzu FLOWSORB 2300). Before the N_2 adsorption, each sample was dried at 373 K for 15 min in a 30% N_2–helium flow. Powder X-ray diffraction (XRD) (Rigaku MultiFlex) was measured using Cu Kα radiation (40 kV and 30 mA) and a carbon monochromater with a scan speed of 4 degrees min^{-1}.

2.5. Oxidative dehydrogenation of methanol

The oxidation of methanol was carried out in a fixed bed microreactor usually at 523–598 K. In a typical reaction, the catalyst (Ru_2Mo_{14}/DC–SiO_2), 20 mg, was held in a reactor made of a Pyrex tube with an inner diameter of 6 mm; the sample was sandwiched between two layers of quartz wool. The catalysts were calcined in an air stream at 623 K for 2 h as mentioned above and then maintained at a desired reaction temperature. The reactant feed was usually a mixture of methanol, O_2 and nitrogen (N_2) in the ratios 5/19/76. This mixture was obtained by passing an O_2/N_2 flow through a methanol saturator maintained in an ice-bath at 273 K. The gas-flow rate was usually kept at 20 $cm^3\ min^{-1}$. The steady state was attained usually at about 0.5–1.0 h after the reactant gas mixture had been exposed to the catalyst, and then catalytic measurements were performed. The compositions of the gas phase before and after the reactor were analyzed by GC (Porapack-T, 1.8 m, Yanako, G1880 and Active carbon, 4 m, G.L. Science, GC320).

3. Results and discussion

3.1. Characterization

Results of elementary and ICP analyses of the product crystals are summarized in Table 1. The temporary molecular weight was determined to be about 1420 on the basis of the weight percents of Na, NH_4^+, Ru and Mo in Table 1. The sum of the masses of oxygen, crystal water and proton in the product is expressed by Eqs. (1) and (2):

Table 1
Chemical component of polyoxomolybdate containing ruthenium

Element	Component (wt.%)	Mole ratio
Ru	7.5	1.0
Mo	46.3	7.0
Na	6.4	4.0
NH_4^+	1.5	1.0

$$S \approx 1420 - (4\mathrm{Na} + \mathrm{NH_4} + \mathrm{Ru} + 7\mathrm{Mo})$$
$$= 1420 - (92 + 18 + 101 + 672) = 537, \quad (1)$$

$$S = 16X + 18Y + Z, \quad (2)$$

where X, Y and Z are the numbers of oxygen atom, crystal water and proton, respectively. The charge valance of the salt of the polyoxomolybdate is expressed by Eq. (3):

$$2X = 7\mathrm{Mo}^{6+} + \mathrm{Ru}^{3+} + 4\mathrm{Na}^{+} + \mathrm{NH_4^+} + \mathrm{ZH}^{+}$$
$$= (42 + 3 + 4 + 1 + Z) = 50 + Z. \quad (3)$$

Substitution of Eq. (3) into Eq. (2) gives Eq. (4):

$$S + 50 = 587 \approx 18(X + Y). \quad (4)$$

The value of the left side $(S + 50)$ is about 587 and is a multiple of 18. Therefore, $S + 50$ must be 576 or 594. The value of 594 is more reasonable than 576 because of the consistency with data in Table 1. From the value of 594, a reasonable combination of oxygen atom, crystal water and proton is determined to be $X{:}Y{:}Z = (25{:}8{:}0)$ or $(26{:}7{:}2)$.

XRD photography for a single crystal of the product (Rigaku AFC5R, Joint Research Center, Kinki University) indicates that its crystal is a monoclinic cell having dimensions of $a = 1.469$ nm, $b = 1.005$ nm, $c = 2.050$ nm and $\beta = 97.89^\circ$; there are four Ru-containing polyoxomolybdate ($RuMo_7$) units in a unit cell. The distance between neighborhood Ru ions was determined to be ca. 0.25 nm by our rough estimation. This value is smaller than that expected from the relatively large lattice constants based on the assumption that Ru ions are located in the center of the $RuMo_7$ unit. These results suggest that the $RuMo_7$ unit is asymmetric and that two Ru ions are centered in the dimer of the $RUMo_7$ unit in the crystal. The results hence support the chemical formula of the product, $Na_8(NH_4)_2[Ru_2Mo_{14}O_{50}]\cdot 16H_2O$ or $Na_8(NH_4)_2H_4[Ru_2Mo_{14}O_{52}]\cdot 14H_2O$. Optimization of the crystal structure of the product will be reported in our next paper.

Powder XRD patterns for the salt of Ru_2Mo_{14} and 37 wt.% Ru_2Mo_{14}/DAPS–SiO_2 are shown in Fig. 1. The pattern of the former is inconsistent with those due to Ru oxides, molybdates and compounds containing Ru and/or Mo stored in an XRD data base [30]. No clear peaks appeared in XRD patterns for Ru_2Mo_{14}/DAPS–SiO_2 samples. The results indicate that the thickness of the loaded Ru_2Mo_{14} on DAPS–SiO_2 is smaller than that satisfying a Bragg condition and that Ru_2Mo_{14} is highly dispersed on the DAPS–SiO_2 support due to the strong interaction between Ru_2Mo_{14} and the protonated amino group in DAPS–TiO_2.

The FT-IR spectra of the salt of Ru_2Mo_{14}, DAPS–SiO_2 and Ru_2Mo_{14}/DAPS–SiO_2 are shown in Fig. 2. The strength of the bands at 945, 900, 756, 690 and 594 cm^{-1} due to Ru_2Mo_7 anion was maintained after loading, though the bands overlap with the bands due to Si–OH and/or Si–O–Si bonds of SiO_2. The FT-IR spectra of samples after thermal treatment of Ru_2Mo_{14}/DAPS–SiO_2 are shown in Fig. 3. Bands at 2950, 2840, 1610 and 1470 cm^{-1} due to DAPS fixed on SiO_2 were observed after thermal treatment at 523 K but disappeared after calcination at 623 K, indicating that the organic moieties of DAPS were removed by calcination at 623 K. The results hence lead to the conclusion that calcination at that temperature eliminates the effects of the organic moieties of DAPS on the catalytic behavior of Ru_2Mo_{14}.

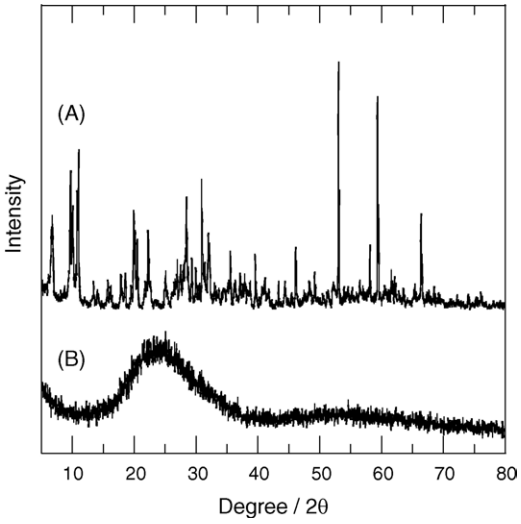

Fig. 1. Powder X-ray diffraction patterns for (A) powder of Ru_2Mo_{14} salt and (B) 37 wt.% Ru_2Mo_{14}/DAPS–SiO_2.

Specific surface areas of SiO_2, DAPS–SiO_2 and Ru_2Mo_{14}/DAPS–SiO_2 samples having various loadings (S_{BET}) are

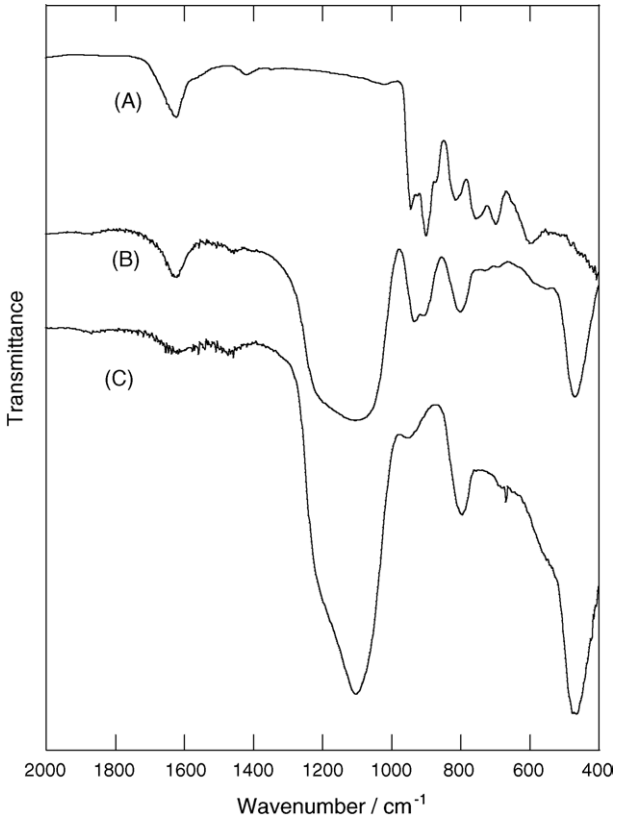

Fig. 2. FT-IR spectra for (A) salt of Ru_2Mo_{14}, (B) 37 wt.% Ru_2Mo_{14}/DAPS–SiO_2 and (C) DAPS–SiO_2.

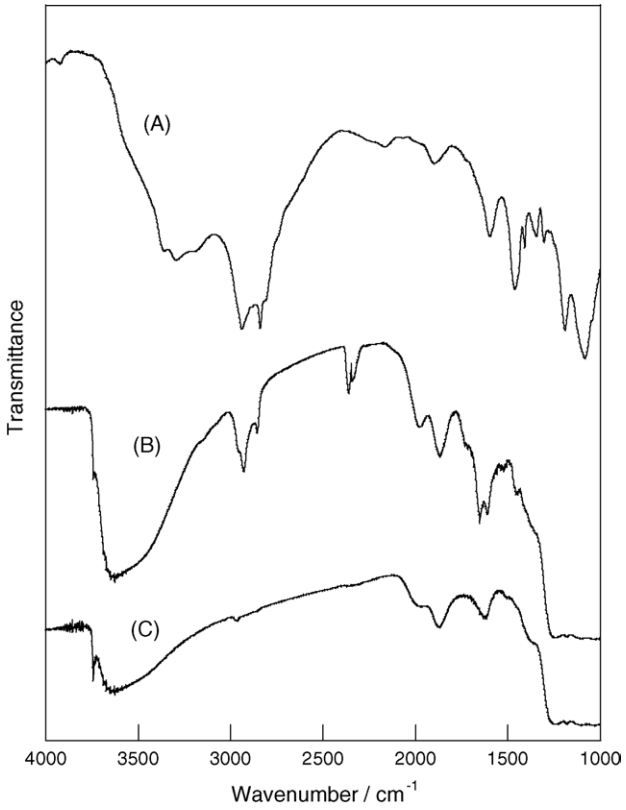

Fig. 3. FT-IR spectra for (A) DAPS and the sample obtained by thermal treatment of Ru_2Mo_{14}/DAPS–SiO_2 at (B) 523 K for 90 min and (C) 623 K for 45 min in vacuo.

summarized in Table 2. From the specific surface areas of Ru_2Mo_{14}/DAPS–SiO_2 samples, surface areas of the loaded Ru_2Mo_{14} species ($S_{Ru_2Mo_{14}}$) were calculated on the basis of the assumption that the surface area of the carrier (DAPS–SiO_2) does not change after Ru_2Mo_{14} loading. The surface areas per Ru_2Mo_{14} unit ($S'_{Ru_2Mo_{14}}$) and its changes with loading were also estimated. In the range of 5–37 wt.%, the surface areas of Ru_2Mo_{14} loaded indicate that the Ru_2Mo_{14} units are quite homogeneously dispersed on the DAPS–SiO_2 carrier. In the minus value of $S_{Ru_2Mo_{14}}$ with more than 50 wt.% loading, the carrier surfaces are thought to be covered completely with Ru_2Mo_{14} units.

Table 2
Surface area of carrier, Ru_2Mo_{14}/DAPS–SiO_2 and loaded Ru_2Mo_{14} species

Entry	W (wt.%)[a]	S_{BET} (m^2 g $cat.^{-1}$)	$S_{Ru_2Mo_{14}}$ (m^2 g $cat.^{-1}$)[b]	$S'_{Ru_2Mo_{14}}$ (nm^2 $unit^{-1}$)[c]
1	(SiO_2)	(266)		
2	(DAPS–SiO_2)	(188)		
3	5	217	38	3.6
4	10	211	42	2.0
5	15	210	50	1.6
6	20	190	40	0.95
7	25	189	48	0.91
8	30	168	36	0.57
9	37	148	30	0.38
10	50	86	−8	
11	60	49	−26	
12	80	24	−14	
13	100 (Ru_2Mo_{14})	<1		

[a] Ru_2Mo_{14} loading.
[b] Calculated from the equation: $S_{BET} - \{S_{BET}(DAPS–SiO_2) \times (100 - W)/100\}$.
[c] Calculated from the equation: $S_{Ru_2Mo_{14}}/\{(1 \times W/(FW_{(Ru_2Mo_{14})})) \times (Avogadro\ number)\}$ where $FW_{(Ru_2Mo_{14})} = 2840$.

3.2. Oxidative dehydrogenation of methanol over Ru_2Mo_{14}/DC–SiO_2

Oxidative dehydrogenation of methanol over the Ru_2Mo_{14}/DC–SiO_2 catalysts was examined in the temperature range of 523–598 K. The methanol conversion increased with elevation of the reaction temperature. Effects of the amount of catalyst and the Ru_2Mo_{14} loading on the methanol conversion and the product distribution at 598 K are summarized in Table 3. Rates of formaldehyde formation are also shown. A combustion reaction of methanol to CO_2 and H_2O occurred over Ru_2Mo_{14} powder and Ru/SiO_2 catalyst. The methanol conversion increased linearly in proportion to the amounts of Ru_2Mo_{14} loaded on the DAPS-modified SiO_2.

The effects of the methanol conversion on the selectivity of formaldehyde and the reaction rate of formaldehyde formation are shown in Fig. 4. Oxidation to formaldehyde proceeded selectively up to ca. 80% of the methanol conversion, whereas decomposition of formaldehyde significantly occurred at a higher rate of conversion. The rate of formaldehyde formation linearly increased up to 41% of methanol conversion; that is, the rate of formaldehyde decomposition is very low even at 598 K, though the decomposition of formaldehyde proceeds rapidly at a higher temperature. Moreover, there was little formation of dimethyl ether at 598 K, though slight formation occurred in entries 11, 12 and 15 in Table 3. Methanol is easily dehydrated to yield dimethyl ether over an acid catalyst. No formation of dimethyl ether was detected in the Ru_2Mo_{14} powder (entry 19). The finding of little formation of dimethyl ether hence supports the idea that there are few sites of strong acid both in the salt of Ru_2Mo_{14} and Ru_2Mo_{14}/DC–SiO_2 catalysts. This suggests that Ru_2Mo_{14} anion is neutralized. At this point, $Na_8(NH_4)_2[Ru_2Mo_{14}O_{50}]\cdot 16H_2O$ may be favorable as the chemical formula of the salt of Ru_2Mo_{14}, although further investigation of the acid properties is required [31].

The results also strongly suggest that formation of CO_2 occurred on Ru_2Mo_{14} bulk and/or Ru metal as a result of the decomposition of Ru_2Mo_7 bulk with heating. As shown in Table 3, formation of CO_2 was observed in the catalysts with high loading of more than 25 wt.%. It is reasonable to assume that aggregation of Ru_2Mo_{14} occurred at loading of more than 25 wt.%. This assumption corresponds to the decrease in the surface area per Ru_2Mo_{14} unit ($S'_{Ru_2Mo_{14}}$) shown in Table 2. These results indicate that loading Ru_2Mo_{14} up to 20 wt.% significantly improves the selectivity of formaldehyde. This means that loading Ru_2Mo_{14} on DAPS–SiO_2 remarkably suppresses the combustion reaction.

Effects of flow rate on the oxidation of methanol were also studied. The results are shown in Fig. 5. The conversion

Table 3
Oxidation of methanol over Ru_2Mo_{14}/DC–SiO_2 and supported Ru catalyst[a]

Entry	Loading (wt.%)	Amount (mg)	CH_3OH conversion (%)	Selectivity (%)				R_{HCHO} (μmol min^{-1})[b]	Specific activity (mmol min^{-1} g^{-1})
				CO	CO_2	HCHO	CH_3OCH_3		
1	0	20	3.5	–	–	100	–	2.3	–
2	5.0	20	9.4	–	–	100	–	6.3	6.3
3	10	20	17	–	–	100	–	11	5.7
4	15	10	22	–	–	100	–	15	9.8
5	15	20	37	4.8	–	95	–	24	7.9
6	20	10	41	7.5	2.9	89	–	24	12
7	20	20	94	12	49	39	–	25	6.1
8	25	10	71	15	4.5	80	–	38	15
9	25	20	100	13	53	34	–	23	4.6
10	30	10	78	12	6.1	82	–	43	14
11	30	20	94	13	36	50	0.6	31	5.2
12	35	10	97	23	17	59	0.4	38	11
13	35	20	92	26	33	40	–	25	3.5
14	37	10	56	8.2	6.5	85	–	32	8.6
15	37	20	93	11	33	55	0.5	34	4.6
16	50	20	95	11	44	45	–	29	2.8
17	60	20	50	4.2	19	77	–	26	2.1
18	80	20	17	–	6.8	93	–	11	0.66
19	100	20	60	–	66	34	–	14	0.68
20	10[c]	20	100	–	100	–	–	–	–

[a] Temperature: 598 K; flow rate: 30 cm^3 min^{-1}; $N_2/O_2/CH_3OH$ = 76/19/5.
[b] Rate for HCHO formation.
[c] Supported Ru catalyst prepared by impregnation of $RuCl_3$ on unmodified SiO_2 carrier and subsequent calcination at 623 K.

decreases with an increase in the flow rate, indicating that the conversion increased in proportion to the reaction time.

The specific activities of the catalysts were determined on the basis of the data in Table 3. As shown in Table 3, the specific activity per weight of Ru_2Mo_{14} was nearly the same in the range of 0–25 wt.%. At 25–35 wt.% loading of Ru_2Mo_{14}, the activity per weight reached maximum. The results support the idea that the cluster of Ru_2Mo_{14} was finely dispersed in the range up to 20 wt.% because the activity per weight was nearly the same: a thick membrane cluster of Ru_2Mo_{14} covers the surface of DAPS–SiO_2 up to 25 wt.% loading and aggregation of the Ru_2Mo_{14} cluster occurs with further loading. Slight aggregation could enhance the activity. The finding of nearly equal activity leads to the conclusion that silane coupling molecules cover the heterogeneous surface of SiO_2 and that modification improves the properties of SiO_2 surface to a chemically uniform state. Therefore, it is concluded that the chemically uniform state of the SiO_2 surface facilitates fine dispersion of the polyoxomolybdate.

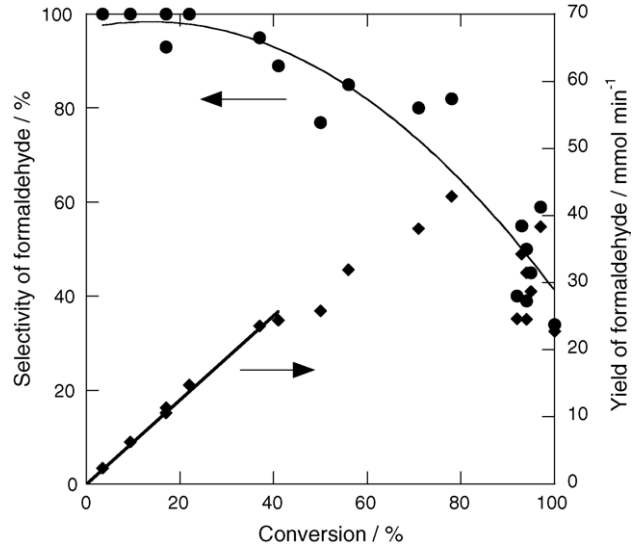

Fig. 4. Effect of the methanol conversion on the selectivity and the yield of formaldehyde. The reaction was carried out under the following conditions: methanol, 5 mol% air valance; temperature, 598 K; flow rate, 30 cm^3 min^{-1}; catalyst, 20 mg.

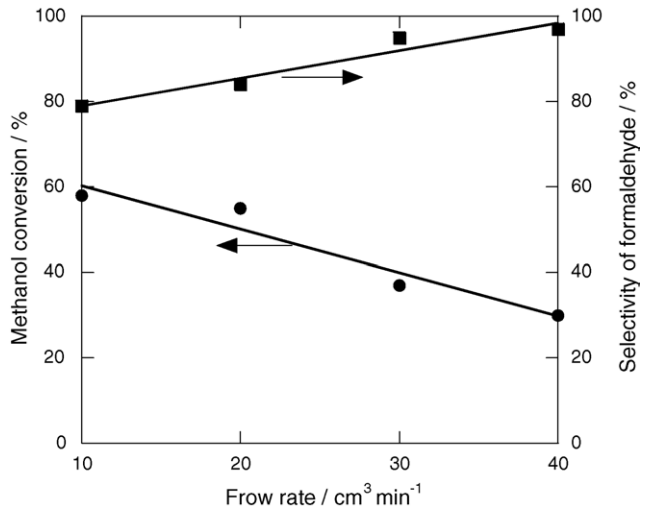

Fig. 5. Effect of flow rate on methanol oxidation (catalyst: 15 wt.% Ru_2Mo_{14}/DC–SiO_2, 20 mg at 598 K).

3.3. Mechanistic aspects on methanol oxidation

FT-IR spectra for methanol and intermediate species on Ru_2Mo_{14}/DC–SiO_2 catalysts were measured. The results are shown in Fig. 6. The bands at 2990 and 2854 cm^{-1} are assigned to a stretching vibration of methanol adsorbed physically [32]. The bands at 2990, 2955, 1458 and 1365 cm^{-1} are assigned to a stretching and bending vibration of $–OCH_3$ groups, and the bands at 3005, 2968, 2912 and 2855, ca.1640, 1447, 1409 and 1373 cm^{-1} are due to formate species, monodentate, bidentate and/or bridging formate, adsorbed on the Ru_2Mo_{14}/DAPS–SiO_2 catalysts [32]. The shoulder band at 1616 cm^{-1} assigned to the –OH group appears upon exposure of the Ru_2Mo_{14}/DC–SiO_2 catalyst at 598 K for 45 min to methanol gas in the absence of O_2. In addition, the band at 1616 cm^{-1} assigned to the –OH group on SiO_2 slightly shifts to a higher wave number and its strength increases. The results can be explained as follows. The formation of H_2O resulting from the oxidative dehydrogenation to formate causes a shift and increase in strength. In addition, the introduction of O_2 to the IR disk rapidly increases the intensity of the bands due to formate species and decreases the intensity of bands at 2854 and 1460 cm^{-1} due to adsorbed methanol. Therefore, the results indicate that dehydrogenation of methanol to formaldehyde occurs in the absence of O_2 and that co-existence of O_2 significantly accelerates the formation of formaldehyde. The formation of formate and/or H_2O species in the absence of O_2 strongly suggests that oxidative dehydrogenation over the Ru_2Mo_{14} occurs using lattice oxygen in Ru_2Mo_{14} and then the introduction of O_2 smoothly fills the vacancies of the used lattice oxygen. The acceleration of formaldehyde formation with O_2 suggests that Ru in polyoxomolybdate increases the mobility of lattice oxygen in the polyoxomolybdate.

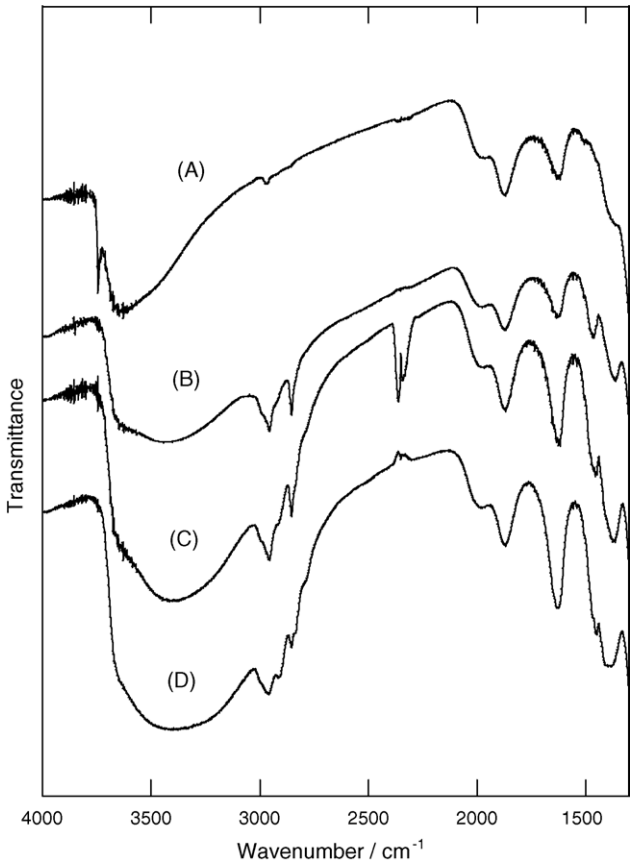

Fig. 6. FT-IR spectra for the species of methanol adsorbed on the catalysts (15 wt.% Ru_2Mo_{14}/DC–SiO_2). (A) Preheated in vacuo at 598 K for 45 min; (B) exposed to methanol at 598 K for 45 min; (C) O_2 was introduced at 598 K for 15 min after (B); (D) O_2 was introduced at 598 K for 45 min after (B).

4. Conclusions

A salt of Ru-containing polyoxomolybdate (Ru_2Mo_{14}) has been prepared and its chemical formula was determined to be $Na_8(NH_4)_2[Ru_2Mo_{14}O_{50}]\cdot 16H_2O$ or $Na_8(NH_4)_2H_4[Ru_2Mo_{14}O_{52}]\cdot 14H_2O$ on the basis of its characteristics and chemical components. Ru_2Mo_{14} is finely dispersed as a mono- and/or bi-layer on the SiO_2 carrier modified with DAPS in the range of 0–20 wt.% loading. The oxidative dehydrogenation of methanol over Ru_2Mo_{14} loaded on the modified SiO_2 carrier selectively gave formaldehyde up to ca. 80% of the methanol conversion, whereas combustion of methanol occurred both over the Ru_2Mo_{14} powder and Ru catalyst. The finding of little formation of dimethyl ether over the Ru_2Mo_{14} powder and the loaded catalysts leads to the conclusion that the fine dispersion of Ru_2Mo_{14} units enhances the selective oxidation of methanol to formaldehyde and that the methanol combustion is caused by the bulky particles of Ru_2Mo_{14} due to a high loading and/or by Ru oxide resulting from the decomposition of Ru_2Mo_{14} units by heating. In addition, the little formation of dimethyl ether indicates that there are few sites of strong acid in the Ru_2Mo_{14} powder and the loaded catalysts. The FT-IR spectra for the adsorbed species on the catalysts support the idea that a hydroxyl group of methanol adsorbs dissociatively on the catalyst and then oxidative dehydrogenation proceeds with lattice oxygen followed by supply of O_2 from a gas phase. The co-existence of O_2 significantly accelerates the formation of formaldehyde. These results suggest that two Ru ions increase the mobility of lattice oxygen in the polyoxomolybdate ($[Ru_2Mo_{14}O_{52}]^{14-}$ or $[Ru_2Mo_{14}O_{50}]^{10-}$).

References

[1] M.T. Pope, Heteropoly and Isopoly Oxometalates, Springer-Verlag, Berlin, 1983.
[2] M. Misono, Catal. Rev. Sci. Eng. 29 (1987) 269.
[3] Y. Ono, Perspectives in Catalysis, Blackwell Science Publications, London, 1992, p. 431.
[4] Y. Izumi, K. Urabe, A. Onaka, Zeolite, Clay, and Heteropolyacid in Organic Reactions, Kodansya-VCH, Tokyo-Weinheim, 1992.
[5] N. Mizuno, M. Misono, J. Mol. Catal. 86 (1994) 319.
[6] C.L. Hill, C.M. Prosser-McCartha, Food Chem. Rev. 143 (1995) 407.
[7] T. Okuhara, N. Mizuno, M. Misono, Adv. Catal. 41 (1996) 113.
[8] I.V. Kozhevnikov, Chem. Rev. 98 (1998) 171.
[9] N. Mizuno, M. Misono, Chem. Rev. 98 (1998) 199.
[10] R. Neumann, Prog. Inorg. Chem. 47 (1998) 317.
[11] M. Kamada, Y. Kera, Chem. Lett. (1991) 1831.

[12] M. Kamada, H. Nishijima, Y. Kera, Bull. Chem. Soc. Jpn. 66 (1993) 3565.
[13] Y. Hanada, M. Kamada, K. Umemoto, H. Kominami, Y. Kera, Catal. Lett. 37 (1996) 229.
[14] M. Kamada, H. Kominami, Y. Kera, Nippon Kagaku Kaishi (1996) 300.
[15] M. Kamada, H. Kominami, Y. Kera, J. Colloid Interface Sci. 182 (1996) 297.
[16] Y. Kera, M. Kamada, Y. Hanada, H. Kominami, Compos. Interfaces 8 (2001) 109.
[17] Y. Kera, T. Oonaka, K. Yamanaka, S. Hirayama, H. Kominami, Appl. Catal. A: Gen. 276 (2004) 187.
[18] R. Shiozaki, A. Inagaki, A. Nishino, E. Nishino, M. Maekawa, H. Kominami, Y. Kera, J. Alloys Compd. 234 (1996) 193.
[19] R. Shiozaki, A. Inagaki, H. Kominami, S. Yamaguchi, J. Ichihara, Y. Kera, J. Mol. Catal. A: Chem. 124 (1997) 29.
[20] Y. Kera, A. Inagaki, Y. Mochizuki, H. Kominami, S. Yamaguchi, J. Ichihara, J. Mol. Catal. A: Chem. 184 (2002) 413.
[21] R. Neumann, M. Dahan, Polyhedron 42 (10) (1998) 3557.
[22] A.M. Khenkin, L.J.W. Shimon, R. Neumann, Inorg. Chem. 42 (10) (2003) 3331.
[23] R. Neumann, C. Abu-Gnim, J. Am. Chem. Soc. 112 (1990) 6025.
[24] R. Neumann, M. Dahan, Nature 388 (6640) (1997) 353.
[25] M. Higashijima, Chem. Lett. 10 (1999) 1093.
[26] J.M. Tatibouët, J.E. Germain, J. Catal. 72 (1981) 375.
[27] J.M. Tatibouët, J.E. Germain, J.C. Volta, J. Catal. 82 (1983) 240.
[28] D.S. Kim, J.M. Tatibouët, I.E. Wachs, J. Catal. 136 (1992) 209.
[29] J.M. Tatibouët, Appl. Catal. A: Gen. 72 (1997) 213.
[30] ICDD database.
[31] K. Brückman, J.M. Tatibouët, M. Che, E. Serwicka, J. Haber, J. Catal. 139 (1993) 455.
[32] L.J. Burcham, M. Bandlani, I.E. Wachs, J. Catal. 203 (2001) 104.